Target dependence of charge distributions in spallation reactions of medium-mass nuclei with 12 GeV protons

T. Asano, Y. Asano, Y. Iguchi, H. Kudo, S. Mori, M. Noguchi, and Y. Takada
Institute of Applied Physics, University of Tsukuba, Sakura, Niihari, Ibaraki 305, Japan

H. Hirabayashi, H. Ikeda, K. Katoh, K. Kondo, M. Takasaki, T. Tominaka, and A. Yamamoto
National Laboratory for High Energy Physics, Oho, Tsukuba, Ibaraki 305, Japan

(Received 15 February 1983)

Spallation yields of Ti, Fe, Co, Ni, Cu, and Zn by 12 GeV protons were measured with a Ge(Li) γ-ray spectrometer followed by computer analysis of the spectra. The measured cross sections of about 30 product nuclides for each target sample are in general agreement with existing data in the same energy range and cover a wider mass range of the product nuclides for most of the targets. The present data were used to obtain the charge-dispersion and mass-yield curves by the least-squares analysis. The target dependence of charge distributions in spallation reactions for product nuclides with a mass range $22 \lesssim A \lesssim 58$ was determined as a function of the N/Z ratio of the target, $(N/Z)_T$. The N/Z ratio at the charge-dispersion peak, $(N/Z)_p$, can be expressed as $(N/Z)_p = (0.783 \pm 0.038) + (0.304 \pm 0.033)(N/Z)_T$. The present results of the target dependence of charge distributions do not seem to agree with the earlier data for production of argon isotopes by 24 GeV protons in the same target mass range.

[NUCLEAR REACTIONS Ti, Fe, Co, Ni, Cu, Zn (p, spallation), $E = 12$ GeV, activation, Ge(Li) detector, cross sections for $7 \lesssim A \lesssim 65$, target N/Z dependence of charge distribution of spallation products.]

I. INTRODUCTION

Spallation reactions of complex nucleus targets with high energy protons have been studied since new accelerators have become accessible in higher energy ranges. In recent years reactions by high energy heavy ions with complex nuclei have also been investigated.[1] Spallation cross sections in high energy nuclear reactions are of great interest in astrophysics as well as in nuclear physics.[2] In addition to physics interest, spallation data are very useful in understanding problems associated with residual radioactivities of various components of high energy accelerators.

The general characteristics of spallation reactions are getting to be well understood phenomenologically. Several attempts have been made to parametrize the currently available data in order to obtain semiempirical formulas that can predict cross sections in the broad mass and energy ranges where measured data are sparse.[3,4]

The target dependence of the relative yields of isobars for spallation reactions was conjectured theoretically and has been observed experimentally. Porile and Church[5] measured strong dependence of the isobaric yield distribution on the N/Z value of the target nucleus using ^{96}Zr, ^{96}Mo, and ^{96}Ru targets with 1.8 GeV protons. Ku and Karol[6] also measured a similar dependence in spallation reactions of ^{92}Mo, ^{96}Mo, and ^{100}Mo with 720 MeV α particles. Recently, the same systematic effects of the target dependence were reported by Regnier[7] for production of argon isotopes in spallation reactions of medium-mass targets in the proton energy range from 0.08 to 24 GeV. Other measurements which suggested the target dependence of spallation products have been reported.[8]

In the present paper we report the results of activation measurements of Ti, Fe, Co, Ni, Cu, and Zn targets with 12 GeV protons. A Ge(Li) detector was used to measure the γ-ray spectra of the irradiated targets. Cross sections for radioactive nuclides for each target were determined from the yields of characteristic γ-ray energies and decay lifetimes of the nuclides. The present results are in general agreement with existing data in the same energy region.[9–19]

The charge-dispersion curves were determined by the least-squares fit to the measured cross sections, and the mass-yield curves were calculated using the parameters obtained in the fit. The parametrization was slightly modified from those studied originally by Rudstam.[3]

Nickel has the smallest N/Z ratio among the targets used in the present experiment. The spallation cross sections for the nickel target are substantially different compared with those for the other targets. These discrepancies can be understood in terms of the target memory effect of the N/Z value of the target. The present data confirm the general features of the target dependence of charge distributions in spallation reactions of medium-mass nuclei in a relatively wide mass range of product nuclides.

II. EXPERIMENTAL PROCEDURE

Stacks of thin metal foils of several different target samples including aluminum were irradiated in the exter-

TABLE I. Arrangements of the target stacks and target thicknesses without including guard foils. The targets starting from the top row in the table were placed starting at the upstream side in the given order. The thicknesses of the stacks are three times the total target thicknesses.

First run		Second run	
Target	Thickness (10^{-3} g/cm^2)	Target	Thickness (10^{-3} g/cm^2)
Al	5.20	Al	3.44
Fe	7.52	Ti	11.0
Co	8.36	Zr	16.6
Ni	17.4	Nb	21.1
Cu	9.06	Mo	14.8
Zn	58.1	Sn	15.2
Ag	12.1	Ta	41.2
Au	39.3	W	48.7
Total	157.0		172.0

nal primary beam line of the 12 GeV proton synchrotron at the National Laboratory for High Energy Physics, Japan (KEK). Exposures of the target stacks were made in two runs two months apart. Table I gives the arrangements of the target stacks and target thicknesses. The numbers of incident protons were 1.57×10^{14} and 2.53×10^{14} in the two exposures of about 10 min. The titanium sample was exposed in the second exposure and the other samples in the first exposure. The 1365.5 keV yields from the ^{24}Na decay of the aluminum samples were used for calibration of the beam intensity monitoring system.[20,21] The ^{27}Al(p,3pn)^{24}Na cross section was measured to be 8.1 ± 0.9 mb at 12 GeV.[21]

Each target sample with natural abundance, ranging in thickness from 8 to 58 mg/cm^2, was guarded by adjacent identical foils in order to minimize scattering-in and scattering-out nuclides by incident protons. The samples with lighter mass nuclei were placed at the upstream end of the stack. The total thickness of each stack was approximately 0.5 g/cm^2. Therefore, the effects due to secondary particles produced in the target stack are expected to be negligible at 12 GeV.

An 85 cm^3 Ge(Li) detector and an 8k-channel pulse-height analyzer system were used for the γ-ray spectroscopy. Measurements were performed at University of Tsukuba. Pulse-height spectra were stored in floppy disks and subsequently transferred to magnetic tapes for the final analysis by a computer.

The detection efficiency of the spectrometer, which corresponds to the photopeak yield for each γ-ray, was measured primarily by several standard checking sources as a function of the γ-ray energy. The efficiency was 1.57% with an energy resolution of 1.6 keV (FWHM) at 1332.5 keV. Above 1400 keV the two γ rays of 1365.5 and 2754.1 keV from the ^{24}Na decay were used and the energy dependence of the efficiency was assumed to be linear in a log-log plot. The estimated uncertainty of the detection efficiency is approximately 15% below 200 keV and 5% above 400 keV.

Measurements started a few hours after the irradiation because of the time required to seal the irradiated samples and because of a short delay for transportation of the samples to the University of Tsukuba. This precluded detection of nuclides with lifetimes shorter than about one hour in the present experiment. Measurements were repeated for the samples sequentially for about three months. About 17 spectra were measured for each sample. The measuring time for each spectrum was increased from 30 min at the beginning of the measurements to several hours.

The γ-ray energies of photopeaks for each spectrum were calibrated to better than 0.2 keV by using clean peaks of the well-established γ rays in the spectrum. A linear relation between the channel and energy was sufficient in the present analysis. Cross sections were determined by the following sequences. First, a candidate nuclide was searched out by looking for photopeak yields associated with its characteristic γ rays. Second, the obtained photopeak yields of several spectra were fitted with its decay time. When more than one nuclide produced γ rays of equal or nearly equal energies, the fit was generally poor. Then, the least-squares fit for two or three nuclides with different decay times was performed to obtain a yield component for the nuclide of interest. Third, when there was more than one γ ray from the nuclide cross sections were computed independently for all the γ rays using their branching ratios. They usually agreed within estimated uncertainties. In general, the accuracies of branching ratio data were better for those with large values near 100%.[22] The detection efficiency and photopeak yields were better determined for higher energy γ rays. Therefore, the final cross section of the nuclide was determined by the result in the most favorable conditions.

III. RESULTS

Measured cross sections are tabulated in Table II. The type of yield of each product nuclide is identified as being either independent (I), or cumulative (C^+ or C^-) when at least one of the precursors is known. When photopeak yields measured were not statistically significant, no cross section values are given. The quoted errors include estimated uncertainties of the detection efficiency of the γ rays and statistical errors for photopeak yields. Since the branching ratios for most of the γ rays used in the analysis are 100% or nearly 100%, uncertainties due to the branching ratios are not included. In most cases the uncertainties of the detection efficiency dominated the overall errors. Systematic uncertainties due to the beam intensity calibration[21] which were estimated to be approximately 10% are not included. Effects due to secondary interactions in the target stacks are estimated to be negligible.

The cross sections for product nuclides much lighter than the target nuclei are very similar for the Fe, Co, Cu, and Zn targets, but they are appreciably different for the Ni target. Large variations in the measured cross sections can be seen for product nuclides with mass numbers very close to the target nuclei. They are caused by isotope abundance of the natural target, and large cross sections

TABLE II. Cross sections (in mb) for Ti, Fe, Co, Ni, Cu, and Zn targets in the nuclear spallation reactions with 12 GeV protons. The second column gives the type of yield, independent (I) or cumulative (C^-: β^- decay, or C^+: β^+ decay or electron capture).

Nuclide	Type of yield	Ti	Fe	Co	Ni	Cu	Zn
^{7}Be	I	7.90±0.43	9.08±0.46	8.00±0.45	12.2±0.7	8.82±0.46	11.4±0.57
^{22}Na	C^+	2.14±0.11	2.35±0.19	1.96±0.16	2.76±0.19	1.95±0.12	1.72±0.10
^{24}Na	C^-	4.12±0.21	3.34±0.19	3.38±0.20	2.80±0.15	3.55±0.18	3.19±0.17
^{28}Mg	C^-	0.58±0.03	0.40±0.03	0.47±0.03	0.26±0.01	0.47±0.025	0.41±0.02
^{38}S	I	0.11±0.01	0.12±0.02			0.14±0.02	0.12±0.01
^{38}Cl	C^-	3.86±0.30					
^{39}Cl	I	0.68±0.05					
^{41}Ar	C^-	1.21±0.06	0.51±0.03	0.69±0.04	0.31±0.03	0.80±0.05	0.61±0.04
^{42}K	I	6.73±0.34	2.94±0.18	3.00±0.18	1.84±0.11	3.54±0.20	2.86±0.17
^{43}K	C^-	2.18±0.11	0.76±0.04	0.99±0.07	0.39±0.02	0.90±0.05	0.76±0.04
^{43}Sc	C^+	2.05±0.12	1.74±0.11	1.27±0.10	2.50±0.21	1.88±0.10	1.81±0.09
^{44}Sc^m	I	2.73±0.14	3.74±0.19	3.47±0.18	3.89±0.20	3.22±0.16	2.96±0.15
^{44}Sc	I	6.90±0.36	2.95±0.15	2.18±0.13	2.95±0.26	2.26±0.12	1.86±0.10
^{46}Sc	I	18.4±0.93	4.99±0.25	5.11±0.26	3.05±0.16	4.68±0.24	4.16±0.21
^{47}Ca	C^-	0.26±0.015				0.10±0.01	0.08±0.005
^{47}Sc	C^-	19.8±3.0	1.98±0.30	2.35±0.35	1.05±0.17	2.13±0.32	1.88±0.28
^{48}Sc	I	1.59±0.08	0.30±0.016	0.45±0.03	0.23±0.014	0.43±0.024	0.42±0.03
^{48}V	C^+	1.21±0.19	8.00±0.41	5.93±0.90	8.82±0.44	5.51±0.28	5.52±0.28
^{48}Cr	I		0.30±0.016	0.16±0.01	0.64±0.04	0.18±0.01	0.19±0.01
^{51}Cr	C^+		21.5±1.1	15.4±0.8	19.1±1.0	13.1±0.7	13.2±0.7
^{52}Mn	I		3.96±0.20	3.36±0.17	5.70±0.29	3.16±0.16	3.44±0.17
^{52}Fe	I		0.25±0.04	0.07±0.01	0.61±0.09	0.09±0.014	0.12±0.02
^{54}Mn	I		27.5±1.4	17.4±0.90	10.3±0.52	12.5±0.6	11.2±0.6
^{55}Co	I		0.15±0.02	0.40±0.03	4.43±0.24	0.56±0.03	0.73±0.04
^{56}Mn	C^-		0.79±0.05	3.22±0.16	0.47±0.06	2.10±0.11	1.42±0.07
^{56}Co	C^+		0.53±0.04	3.27±0.18	18.8±0.9	3.67±0.20	3.93±0.20
^{56}Ni	C^+				1.19±0.06		
^{57}Co	C^+		0.32±0.05	17.0±2.6	47.3±7.1	13.1±2.0	14.0±2.1
^{57}Ni	C^+			0.11±0.01	16.6±0.8	0.43±0.03	0.71±0.04
^{58}Co	I			38.8±1.9	12.0±0.6	17.5±0.9	15.4±0.8
^{59}Fe	I			0.38±0.03	0.46±0.05	1.51±0.08	1.13±0.06
^{60}Co	I					7.83±0.46	4.49±0.23
^{61}Cu	C^+					7.07±0.36	8.62±0.46
^{62}Zn	C^+					0.21±0.016	3.59±0.19
^{65}Ni	I						0.66±0.05
^{65}Zn	C^+					0.83±0.06	20.3±1.0

for peripheral proton-nucleus interactions in which the target nucleus loses only a few nucleons.[23–25]

The present Cu data are in general agreement with those measured by Cumming *et al.*[9,10] with 3.9 and 28 GeV protons. The present data tend to be smaller by about 10% than the 28 GeV data. The largest discrepancy between the present data and the 28 GeV data is about 30% for a few nuclides. The present results are also in qualitative agreement with those measured by Hudis *et al.*[11] in the proton energy range between 3 and 30 GeV.

Brodzinski *et al.*[12,13] measured spallation cross sections for Ti and Fe targets in the proton energy range between 15 and 584 MeV and showed the energy dependence of the cross sections for various product nuclides including the data which had been previously reported.[14] The present data are quite consistent with the extrapolated values at 12 GeV. Production cross sections of ^{7}Be and ^{22}Na from Fe and Ni targets measured by Raisbeck and Yiou[15] with 1, 2, 3, and 23 GeV protons are also reasonably consistent with the present results. Chackett's data[16] for production cross sections of ^{42}K and ^{43}K from Fe, Co, Ni, Cu, and Zn at 18.3 GeV agree reasonably well with the present data. They are also in partial agreement with Rayudu's data[17] for Fe and Ni in the proton energy range from 0.5 to 2.9 GeV, and with Perrons' data[18] for Fe with 21 GeV protons.

The cross section of ^{48}Ti(p,2p)^{47}Sc measured by Jacob and Markowitz[19] using an enriched ^{48}Ti target above 0.3 GeV agrees well with the present cross section for ^{47}Sc production from Ti. (The abundance of ^{48}Ti in natural titanium is 74%.)

IV. ANALYSIS AND DISCUSSION

A. Least-squares analysis

Following the work by Cumming *et al.*[10] and by Porile *et al.*[26] the cross section was parametrized by a modified

TABLE III. Results of the analysis of charge-dispersion curves and target parameters.

Item	Ti	Fe	Co	Ni	Cu	Zn
A_{min}	22	28	28	28	28	28
A_{max}	43	52	52	52	58	58
Number of nuclides	10	14	13	13	22	22
Z_p/A	0.4649±0.0043	0.4688±0.0013	0.4657±0.0014	0.4722±0.0006	0.4658±0.0004	0.4668±0.0005
$(N/Z)_p$	1.151±0.020	1.133±0.006	1.147±0.006	1.118±0.003	1.147±0.002	1.142±0.002
N_T	25.93	29.91	32.00	30.77	34.62	35.47
$(N/Z)_T$	1.179	1.151	1.183	1.099	1.194	1.183

form of the Rudstam equation,[3]

$$\sigma(A,Z)=\exp[(a_1+a_2A+a_3A^2)+(a_4+a_5A)\,|\,Z_p-Z\,|^{1.5}] \quad (1)$$

and

$$Z_p=a_6A\ , \quad (2)$$

where Z_p is the most probable charge, and Z and A are the atomic and mass numbers of spallation products, respectively. Since cross sections for nuclides very close to the target mass number depend strongly on nuclear reactions of individual target isotopes, the data for those nuclides are not included in the analysis. Very light nuclides are not included because only a few nuclides were measured in the mass range below $A=28$ and because it is difficult to fit the data for those nuclides with the simple parametrization by Eqs. (1) and (2).

In the exponent of Eq. (1) the three components $a_1+a_2A+a_3A^2$, a_4+a_5A, and Z_p-Z, have almost orthogonal relations to each other. They correspond to the magnitude of the mass yield, the width of the charge-dispersion curve, and the most probable charge for a mass number A, respectively. Although the width of the charge-dispersion curve can also be adjusted by the value of the power of $|Z_p-Z|$, we present the results for the value of 1.5. Equally good fits to the data were obtained for different values after optimizing a_4 and a_5. In the least-squares fit minimization of the chi-square value was made independently for the three components and repeated sequentially.

The analysis consists of three steps. In the first step we assumed all the cross sections to be independent yields and to have 20 to 30% errors. It was always difficult to get physically meaningful fits to the data with the original errors, which were typically better than 10%. In the second step we computed cross sections for all the isobars of measured nuclides using the parameters obtained in the first step. Then, the measured cumulative cross sections were adjusted proportionally to the computed ratios of the cross sections. The least-squares fit was carried out for the adjusted cross sections, and a new set of adjusted cross sections was calculated. This procedure was repeated until a good fit was obtained. In the third step the least-squares fit was carried out only for the first component, $a_1+a_2A+a_2A^2$, using a partial data set which satisfied $|Z_p-Z|<1.0$ for Z_p obtained in the second step. This method was used to obtain better mass yield curves nearly independently of data for very small cross sections away from the charge-dispersion peak.

B. Charge-dispersion curves

Results of the fit are given in Table III together with the mass range and the number of data points of product nuclides used in the analysis. The ^{52}Mn data were not included in the analysis due to lack of information on ^{52}Mn^m production. The errors given correspond to the standard errors which were calculated after adjusting errors of the cross section data uniformly so that the chi-square value of the best solution was equal to the degree of

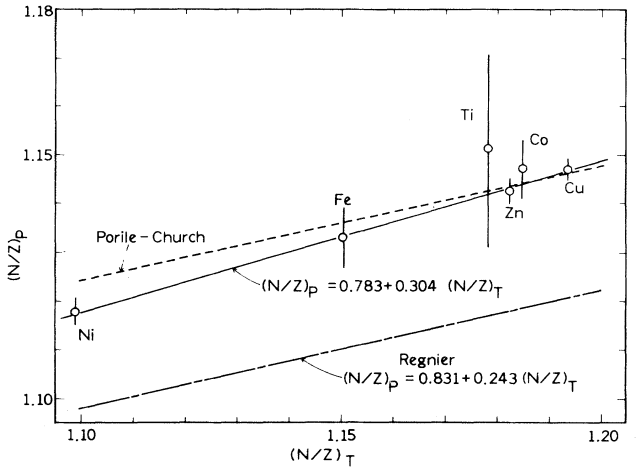

FIG. 1. $(N/Z)_p$ ratio at the charge-dispersion peaks as a function of the $(N/Z)_T$ ratio of the target. The solid line is the best linear fit. The dashed line represents a linear extrapolation of the data of Porile and Church (Ref. 5) and the dashed-dotted line is Regnier's result (Ref. 7).

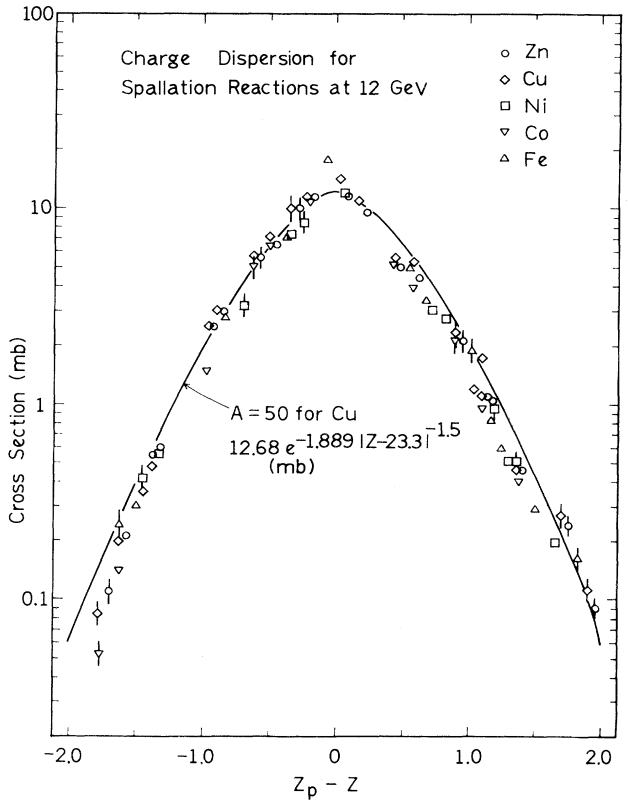

FIG. 2. Charge-dispersion curve for product nuclides in the mass range $28 \leq A \lesssim 58$ in nuclear spallation reactions of Fe, Co, Ni, Cu, and Zn targets with 12 GeV protons. The original cross sections were corrected by subtracting yield contributions from the short-lived parent nuclides and then normalized to the cross section at a fixed mass (see the text). The solid curve corresponds to the fitted charge-disperison curve for Cu at $A=50$. The errors are drawn only when they are large enough to be visible.

freedom. The adjusted errors of the cross sections were about 25% for all the targets. The error for Ti was large due to fewer data points. Also given in Table III are the average number of neutrons of the target, N_T, and the average N/Z ratio of the target, $(N/Z)_T$.

The mass dependence of Z_p/A was evaluated by the least-squares analysis using the parametrization of $Z_p = a_6 A + a_7 A^2$. The quality of the fit was not improved for all the targets. Therefore, the mass dependence of Z_p/A must be insignificant in the mass range analyzed.

The values of the N/Z ratio at the charge-dispersion peaks, $(N/Z)_p$, were calculated from the fitted Z_p/A values and are shown in Fig. 1 with $(N/Z)_T$. The target dependence of $(N/Z)_p$ is clearly seen. The Ni target has the smallest $(N/Z)_p$ and $(N/Z)_T$ values. The solid curve is the best linear fit to the data and is given by the relation

$$(N/Z)_p = (0.783 \pm 0.038) + (0.304 \pm 0.033)(N/Z)_T \ . \quad (3)$$

The dashed line represents a linear extrapolation from Porile and Church's results[5] for ^{96}Zr, ^{96}Mo, and ^{96}Ru with 1.8 GeV protons. Although the data have a limited statistical accuracy, they are consistent with the present results. The dashed-dotted line is a linear correlation obtained by Regnier[7] for production of argon isotopes of 24 GeV from targets in the same mass range as in the present work. It does not agree with the present results. The data of Ku and Karol[6] with 720 MeV α particles do not seem to agree with the present results.

Although there exist large discrepancies among the various experiments, the slopes of the linear approximations between $(N/Z)_p$ and $(N/Z)_T$ seem to be in reasonable agreement with each other and they are about 0.3. If the composition of the target remains proportional in the target fragments of the spallation reactions, then the slope should be unity. Therefore, the experimental results indicate that nuclear spallation processes seem to retain the charge composition of the target rather weakly.

A plausible explanation for this effect is as follows. At the early stage of the evaporation process the ratio of the numbers of neutrons to protons out of the target nucleus is approximately equal to $(N/Z)_T$. When the nucleus cools down, the Coulomb barrier suppresses emission of protons. Therefore, the N/Z ratio for product nuclides becomes slightly smaller than $(N/Z)_T$. In the case of Ni the N/Z ratio becomes somewhat larger than $(N/Z)_T$ after the early evaporation process because of an unusually small N/Z ratio of the target nucleus. The Coulomb suppression does not quite compensate for this increase. Thus, $(N/Z)_p$ is slightly larger than $(N/Z)_T$ for Ni, as is seen in Fig. 1.

Figure 2 shows normalized cross sections with respect to the charge dispersion curve as a function of $Z_p - Z$. The original cross sections were corrected by adjusting the yield contributions from short-lived isobaric parent nuclides which were calculated by the parameters obtained in the second step. Adopting the procedure by Porile

et al.,[26] the corrected cross sections were normalized by

$$\sigma'(A,Z)=\sigma(A,Z)\frac{\sigma(A_0,Z_{p0})}{\sigma(A,Z_p)}\ , \tag{4}$$

where A_0 is 46 for Fe, Co, and Ni and 50 for Cu and Zn, and Z_{p0} is the most probable charge for A_0. Hence, $\sigma(A_0,Z_{p0})$ is the peak isobaric cross section at A_0. The solid curve is the fitted charge-dispersion curve for Cu at $A=50$. The parameters used are $a_1=-2.87$, $a_2=0.180$, $a_3=-1.43\times10^{-3}$, $a_4=-1.89$, $a_5=2.0\times10^{-4}$, and $a_6=0.466$. Fitted curves are essentially identical for all the targets except for Ti which has a slightly broader curve. It should be noted that the A dependence of the width of the charge-dispersion curves is not significant in the mass range studied in the present analysis, and that equally good fits were obtained without the parameter a_5. In order to fit the data in the mass range given in Table III, the three normalization parameters a_1, a_2, and a_3 were required.

C. Mass yield

The mass yield is calculated by

$$\sigma(A)=\sum_Z \sigma(A,Z)\ , \tag{5}$$

and the mass-yield curve is determined predominantly by cross section data near the charge-dispersion peaks. On the other hand those away from the charge-dispersion peaks are important for determining the most probable charge Z_p and the widths of the charge-dispersion curves. Therefore, the final optimization of the mass-yield curve was made for the data with $|Z_p-Z|<1$ in the third step of the analysis. As can be seen in Fig. 2, the corrected cross sections are quite consistent for all the targets. Figure 3 shows the corrected mass-yield data for the Cu and Zn targets. The errors shown correspond to the same fractional errors of the original cross section data. The solid curve corresponds to the smoothed mass-yield curve calculated for Cu. In general, the mass-yield curve calculated by Eqs. (1) and (5) has a small fluctuation of about 10% as a function of A. The computed yield has a large value when Z_p is nearly an integer and it has a small value when Z_p is nearly half an integer. Hence, the fit to the data in the present analysis seems to be adequate. The dashed and broken lines are fitted mass-yield curves obtained by Cumming *et al.*[9,10] for Cu at 3.9 and 28 GeV. The present result is in reasonable agreement with the 28 GeV curve.

The mass-yield curves obtained by Husain and Katcoff[27] for V at 3 and 29 GeV are also in qualitative agreement with the present results.

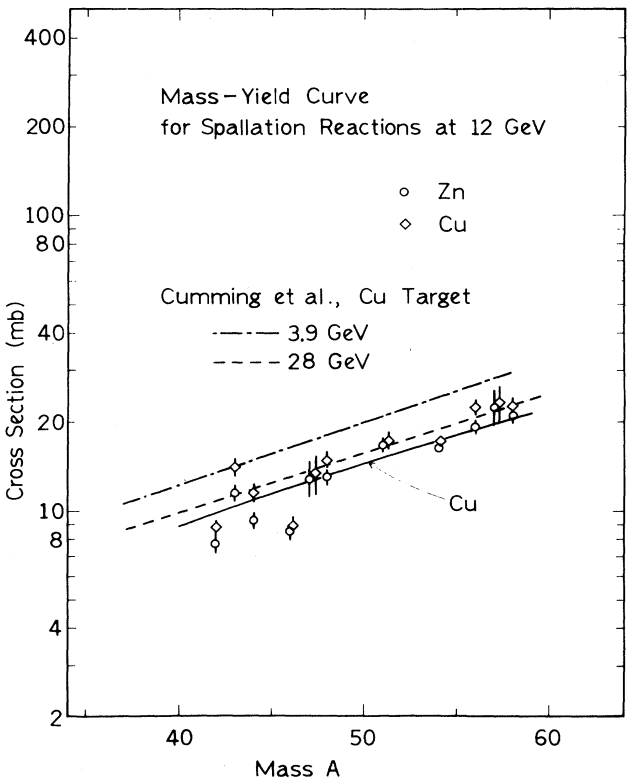

FIG. 3. Mass yield for Cu and Zn. The solid curve corresponds to the smoothed mass-yield curve calculated for Cu. The dashed and dotted-dashed lines are mass-yield curves obtained by Cumming *et al.* (Refs. 9 and 10) for Cu at 3.9 and 28 GeV. The data points shown are for the product nuclides which fall in $|Z_p-Z|<1$ in the charge-dispersion curve.

V. CONCLUSION

A clean target dependence of the charge-dispersion peak Z_p was observed. The composition of the target was manifested qualitatively in target fragments, but the effect is rather weaker in spallation reactions than that expected from the direct proportionality of the target charge ratio. Although the present results do not agree with some of the previous observations,[5–8] the slopes of the linear approximations between $(N/Z)_p$ and $(N/Z)_T$ seem to be in reasonable agreement with each other. Essentially no mass dependence of Z_p/A was observed in the mass range analyzed for all the targets.

Corrected cross sections are quite consistent for all the targets and no target dependence of the mass-yield curve was observed.

ACKNOWLEDGMENTS

We would like to thank the staffs at KEK for their support, Dr. Y. Kawada and Dr. M. Kimura for providing us checking sources, and Professor I. Miura for his support and encouragement in the present work. We would also like to thank Mr. S. Dohi for maintenance of the detection system.

[1]P. E. Hodgson, *Nuclear Heavy-Ion Reactions* (Clarendon, London, 1978), Chap. 10.
[2]For example, see *Spallation Nuclear Reactions and Their Applications,* edited by B. S. P. Shen (Reidel, Boston, 1976).
[3]G. Rudstam, Z. Naturforsch. 21a, 1027 (1966).
[4]R. Silberberg and C. H. Tsao, Astrophys. J. Suppl. 25, 313 (1973); 25, 335 (1973).
[5]N. T. Porile and L. D. Church, Phys. Rev. 133, B310 (1964).
[6]T. H. Ku and P. J. Karol, Phys. Rev. C 16, 1984 (1977).
[7]S. Regnier, Phys. Rev. C 20, 1517 (1979).
[8]S. Kaufman, Phys. Rev. 129, 1866 (1963).
[9]J. B. Cumming, P. E. Haustein, R. W. Stoenner, L. Mausner, and R. A. Naumann, Phys. Rev. C 10, 739 (1974).
[10]J. B. Cumming, R. W. Stoenner, and P. E. Haustein, Phys. Rev. C 14, 1554 (1976).
[11]J. Hudis, I. Dostrovsky, G. Friedlander, J. R. Grover, N. T. Porile, L. P. Remsberg, R. W. Stoenner, and S. Tanaka, Phys. Rev. 129, 434 (1963).
[12]R. L. Brodzinski, L. A. Rancitelli, J. A. Cooper, and N. A. Wogman, Phys. Rev. C 4, 1250 (1971).
[13]R. L. Brodzinski, L. A. Rancitelli, N. A. Wogman, and J. A. Cooper, Phys. Rev. C 4, 1257 (1971).
[14]N. T. Porile and S. Tanaka, Phys. Rev. 135, B122 (1964).
[15]G. M. Raisbeck and F. Yiou, Phys. Rev. C 12, 915 (1975).
[16]K. F. Chackett, J. Inorg. Nucl. Chem. 27, 2493 (1965).
[17]G. V. S. Rayudu, J. Inorg. Nucl. Chem. 30, 2311 (1968).
[18]C. Perron, Phys. Rev. C 14, 1108 (1976).
[19]N. P. Jacob, Jr. and S. S. Markowitz, Phys. Rev. C 11, 541 (1975).
[20]J. B. Cumming, V. Agoritsas, and R. Witkover, Nucl. Instrum. Methods 180, 37 (1981).
[21]H. Hirabayashi *et al.*, J. Phys. Soc. Jpn. 51, 3098 (1982).
[22]*Table of Isotopes,* 7th ed., edited by C. M. Lederer and V. S. Shirley (Wiley, New York, 1978).
[23]N. T. Porile and S. Tanaka, Phys. Rev. 130, 1541 (1963).
[24]J. C. Hill, G. Shirk, R. F. Petry, and K. H. Wang, Phys. Rev. C 12, 1978 (1975).
[25]M. A. Molecke and A. A. Caretto, Jr., Phys. Rev. C 15, 719 (1977).
[26]N. T. Porile, G. D. Cole, and C. R. Rudy, Phys. Rev. C 19, 2288 (1979).
[27]L. Husain and S. Katcoff, Phys. Rev. C 7, 2452 (1973).